Population kinetics of lithiumlike ions in plasma

Tetsuya Kawachi and Takashi Fujimoto
Department of Engineering Science, Kyoto University, Kyoto 606-01, Japan
(Received 25 April 1994)

For lithiumlike ions (oxygen and aluminum), characteristics of the population distribution over the excited levels and the population kinetics are examined in detail. In the high-density region, a simple approximate distribution function is derived for both the ionizing and recombining plasma components on the basis of the multistep ladderlike excitation or deexcitation mechanism, combined with the thermodynamic equilibrium distribution. As examples of applications, we present intensity ratios of emission lines from impurity ions in hydrogen plasma, and the population inversion and gain for the x-ray recombining plasma laser.

PACS number(s): 52.70.−m

I. INTRODUCTION

Population distribution among excited atoms and ions in a plasma reflects the nature of the plasma concerned, and is the subject of plasma spectroscopy through observation of the spectrum emitted by the these atoms and ions. A wide variety of population characteristics, e.g., thermodynamic equilibrium and population inversion, could be realized depending on various collisional and radiative processes in the plasma. A comprehensive investigation of the general characteristics of the population and its kinetics was reported 15 years ago [1].

Reference [1] treats atomic hyderogen as a typical example of atomic and ionic species. It divides an excited level population into an ionizing plasma component and a recombining plasma component. It then proposes a classification scheme for the population distribution into several categories: the corona phase and the ladderlike excitation-ionization phase for the ionizing plasma component, and the capture-radiative-cascade phase, local thermodynamic equilibrium (LTE) phase and ladderlike deexcitation phase for the recombining plasma component. Depending on the particular condition of the plasma in question, one of these phases, or two or even three of them, would manifest itself in the observed spectrum.

The above treatment, however, is rather limited in several respects. The first is the energy level structure of hydrogen. The ionization potential of the ground state is four times that of the first excited state, or the ground state potential is rather deep. This feature is shared by heliumlike ions, which have an even deeper ground state, but is rather exceptional for many atomic and ionic species which have shallow potentials. A second weakness is that $s,p,d,\ldots$ states, or different l levels, are bundled together, or that they are assumed to be populated according to their statistical weights. This assumption obviously breaks down in low-density plasmas in which collisional population mixing among these levels is slower than radiative decay. It is even not entirely clear whether this assumption is valid in high-density ionizing plasmas, since they are not in equilibrium in nature. In view of these limitations and questions, it was decided to extend the investigation of the population characteristics to atoms and ions having a rather shallow potential, and with the above assumption removed.

Lithiumlike ions have the next simpler energy level structure to hydrogen, and it is feasible to construct a reliable collisional-radiative model with the different l levels resolved. We can even resolve the fine structure components. We have completed this attempt, and its details are described in our previous paper [2].

In this paper, we investigate the characteristics and kinetics of excited level populations in lithiumlike ions for both ionizing and recombining plasma components, and examine how those established for hydrogen are valid, modified, or even replaced for the nonhydrogenic case. We also show examples of our calculation which are relevant to actual plasmas, i.e., tokamak plasma and recombination plasma for x-ray laser.

II. POPULATION KINETICS

In the collisional-radiative model, the population of excited level p of the lithiumlike ion is given by

$$n(p)=R_0(p)n_e n_{\mathrm{He}}+R_1(p)n_e n_{\mathrm{Li}}\ ; \tag{1}$$

that is, the sum of the ionizing plasma component proportional to the ground state density n_{Li} and the recombining plasma component proportional to the heliumlike ion density n_{He} [1]. n_e is the electron density. These components are expressed by the population coefficients $R_1(p)$ and $R_0(p)$. The validity of Eq. (1) has been discussed in [2]. In the following, we examine these components separately.

A. Ionizing plasma component

We take the O VI ion as an example. Figure 5 of [2] shows the n_e dependence of the population of some of the excited levels. The electron temperature T_e is assumed to be 50 eV; this T_e corresponds to that of tokamak plasmas, where the O VI ions in this ionization stage are present predominantly.

In the low-density region of $n_e<10^{14}$ cm^{-3} [$\eta<10^9$

cm^{-3}; η is the reduced or equivalent density for neutral isoelectronic species and is defined as $\eta = n_e/(z-2)^7$, where z is the nuclear charge], the populations of low-lying excited levels with $n \leq 10$ are proportional to n_e; these levels are in the corona phase, as explained below and the magnitude of the populations of the different l levels per unit statistical weight is in the order $s, p, d, \ldots$ for the $n = 3$, 4, and 5 levels. For higher-lying excited levels with $n > 10$, deviation from the linear relation has already taken place. In the region of 10^{15} $cm^{-3} < n_e < 10^{18}$ cm^{-3} (10^{10} $cm^{-3} < \eta < 10^{13}$ cm^{-3}), a deviation from the linear relation occurs for the low-lying levels. At the same time, the populations in the different l levels tend to be proportional to their statistical weights. In the high-density region, $n_e > 10^{18}$ cm^{-3} ($\eta > 10^{13}$ cm^{-3}), all populations reach their high-density limit values.

We examine the n_e-dependent populations in more detail. We take the $4\,^2P$ level as an example: Figs. 1(a) and 1(b) show the magnitude of the population flows into and out of this $4\,^2P$ level. For convenience, the population flow has been divided by n_e, and the values in the high-density limit are given by numbers. In the low-density region, the dominant flow into this level is the direct excita-

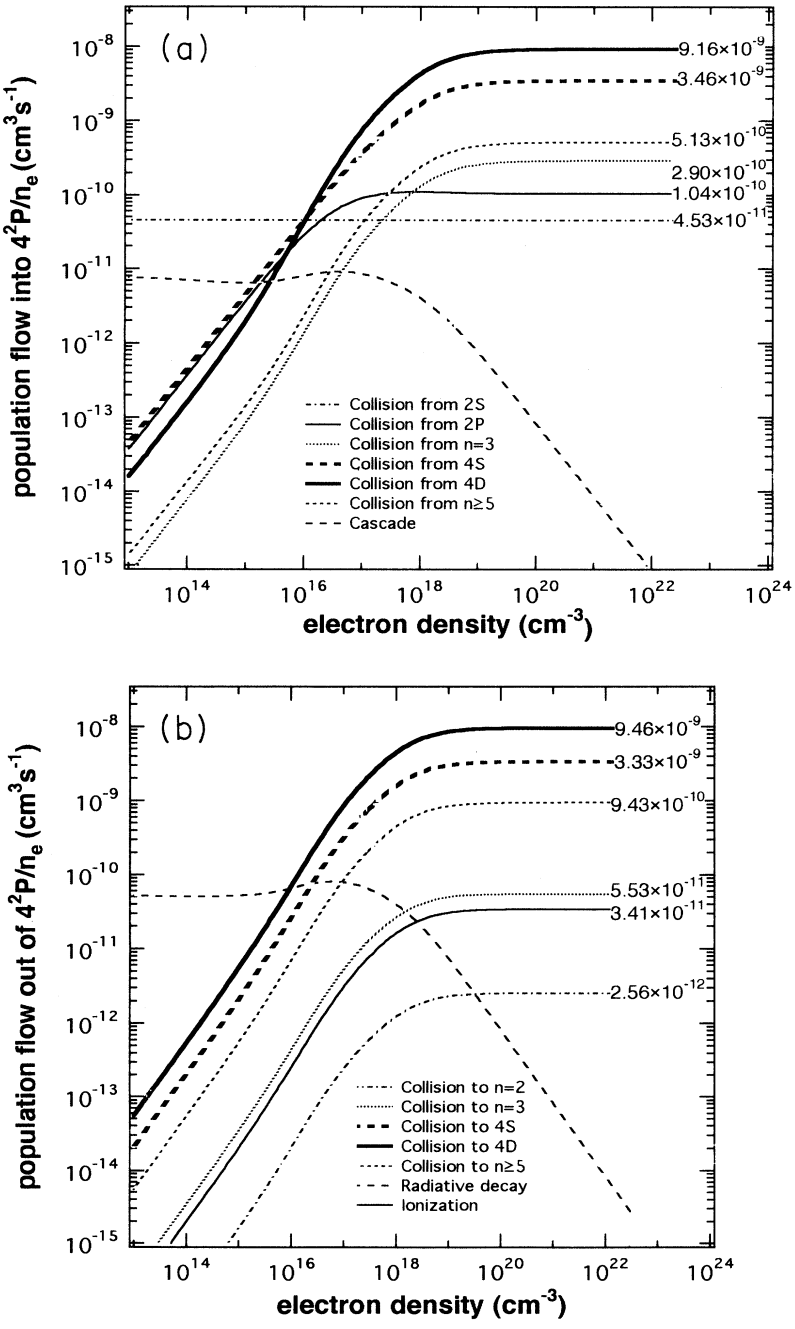

FIG. 1. Population flows (a) into and (b) out of the $4\,^2P$ level for the ionizing plasma component in Fig. 5 in [2]. The magnitude of the flow has been divided by electron density for convenience. The number attached on the right side is the magnitude at the high-density limit.

tion from the ground state $2\,^2S$, and a contribution from cascade from higher-lying levels is about 20%. This value is typical for low-density ionizing plasmas, as Appendix A shows. The dominant flow out of $4\,^2P$ is the radiative decay, 80% of which is the transition to the ground state. This is consistent with the linear relationship in Fig. 5 of [2] in this region and the nomenclature of the corona phase. At about $n_e = 10^{15}$ cm^{-3}, the contribution from the excitation from $2\,^2P$ begins to be substantial. At the same time, the l-changing transitions by proton collisions become substantial. These additional contributions result in the slight upward deviation of the population from the linear relation in Fig. 5 of [2]. [See also in Fig. 1(b) the slight increase in the radiative decay flow which is proportional to the population.] In $n_e > 10^{16}$ cm^{-3}, the population of the $2\,^2P$ level becomes almost equal to or even larger than that of the $2\,^2S$ state. [Remember that the population in Fig. 5 of [2] has been divided by the statistical weight; $g(2\,^2S)=2$, $g(2\,^2P)=6$.] The population flow from $2\,^2P$ into $4\,^2P$ becomes larger than that from the ground state $2\,^2S$. In such a situation, the $2\,^2S$ and $2\,^2P$ levels altogether may be regarded as the ground level.

In this higher density region $n_e > 10^{16}$ cm^{-3}, the dominant flows both into and out of $4\,^2P$ are l-changing collisions $4\,^2S \leftrightarrow 4\,^2P$ and $4\,^2P \leftrightarrow 4\,^2D$ (see Table I of [2]). It might be assumed that, in the high-density limit, the populations of $4\,^2S$, $4\,^2P$, $4\,^2D$, and $4\,^2F$ are in thermodynamic equilibrium, or almost equivalently determined by their statistical weights. In Figs. 1(a) and 1(b), the population flow from $4\,^2S$ to $4\,^2P$ is larger than the inverse flow by 4%, and the flow from $4\,^2P$ to $4\,^2D$ is larger than the inverse flow by 3%. This means that there exists a small but substantial net upward flow of $4\,^2S \Longrightarrow 4\,^2P \Longrightarrow 4\,^2D \Longrightarrow 4\,^2F$, so that these levels are never in thermodynamic equilibrium. This flow may be called the generalized ladderlike excitation-ionization established among the different l levels with the same n. The population flows of $n=3 \rightarrow n=4$ and $n=4 \rightarrow n=5$ is about one order of magnitude smaller than the individual l changing flow, but is larger than the net l-changing flow. Figure 2 shows the population distribution at the high-density limit or $n_e = 10^{20}$ cm^{-3}. The abscissa is the effective principal quantum number p^* of the levels in a logarithmic scale. The ordinate is the reduced population coefficient $r_1(p)$ which is related to the population coefficient as

$$r_1(p) = \frac{R_1(p)g(1)}{g(p)} \exp\left[\frac{E(p)}{kT_e}\right], \tag{2}$$

where $E(p)$ is the energy of level p measured from the ground state. In the case of the ground state $2\,^2S$, $r_1(2\,^2S)$ is set equal to 1. If thermal equilibrium were established among a group of levels, $r_1(p)$ for these levels would be equal. On the contrary, for $n=2$, 3, 4, and 5 levels, the different l levels have different r_1's, being consistent with the above statement. Therefore, for hydrogen or hydrogenlike ions, the question is still open whether different l levels with same n are populated according to their statistical weights or not under the high-density conditions [3].

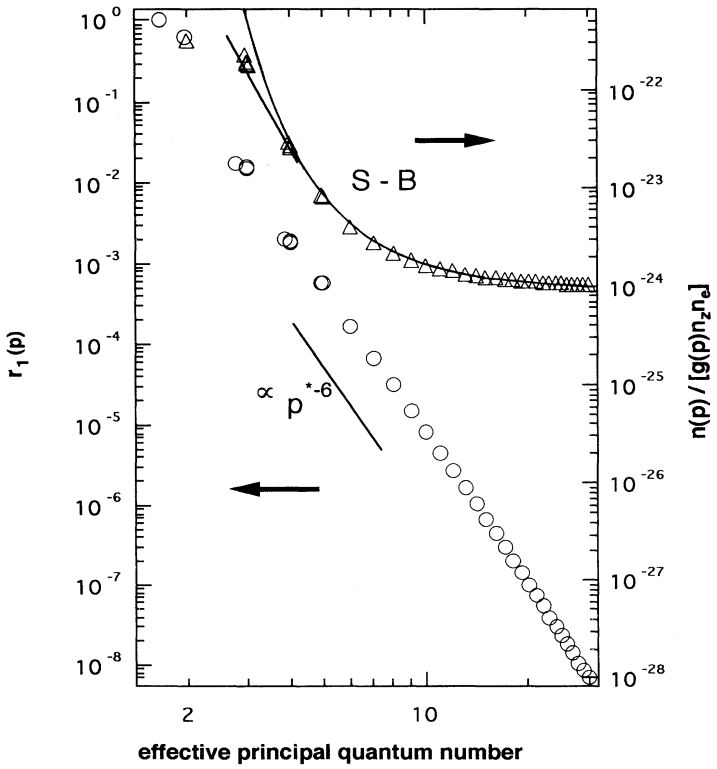

FIG. 2. Population distribution against the effective principal quantum number for both the ionizing plasma component (open circle) and the recombining plasma component (open triangle). The solid curve (SB) denotes the Saha-Boltzmann distribution. The straight lines have a slope -6, indicating the ladderlike excitation or deexcitation.

Figure 2 shows that $r_1(p)$ has a monotonic p dependence and is given approximately by

$$r_1(p) \propto p^{*-6} \tag{3}$$

starting from $r_1(2\,^2S)=1$.

The p^{*-6} dependence was first shown theoretically for neutral hydrogen [1,4], and verified experimentally for neutral argon [5] and for helium [6]. This dependence is the result of the establishment of the ladderlike excitation-ionization process together with the characteristic that the approximate relationship of the excitation rate coefficients $C(p,p+1) \propto p^4$, where p is understood to denote the principal quantum number. It is interesting also to find here a similar relation in the case of a highly charged ion. The slight failure of Eq. (3) between $n=2$ and 3 is the result of the failure of the above approximation of the excitation rate coefficients. The different l levels show a slope intermediate between Eq. (3) and thermodynamic equilibrium.

The relationship expressed by Eq. (3) suggests a method of estimating the excited-level populations in ionizing high-density plasmas; i.e., if we know a low-lying level population or even the ground-state population, we can derive approximate populations of the excited levels from Eq. (3).

Figure 3 shows the photon emission ratio of transitions $2\,^2S-3\,^2P$ to $2\,^2P-3\,^2S$ and that of $2\,^2P-3\,^2D$ to $2\,^2P-3\,^2S$ of C IV, N V, and O VI ions against electron temperature. We assume a hydrogen plasma with $n_e=10^{13}$ cm^{-3}, which is typical for a tokamak plasma where these ions are present. In such a low-density plasma, there is no significant density effect on the $n=3$ level populations. The two sets of results correspond to the two different cross section data for $2\,^2S-3\,^2P$, as shown in Fig. 2 in [2]. A similar calculation result by Zastrow *et al.* [7] is also given. The slight difference between the two calculations could be explained as due to the cascade contribution from the $n \geq 6$ levels, which is neglected by Zastrow *et al.*

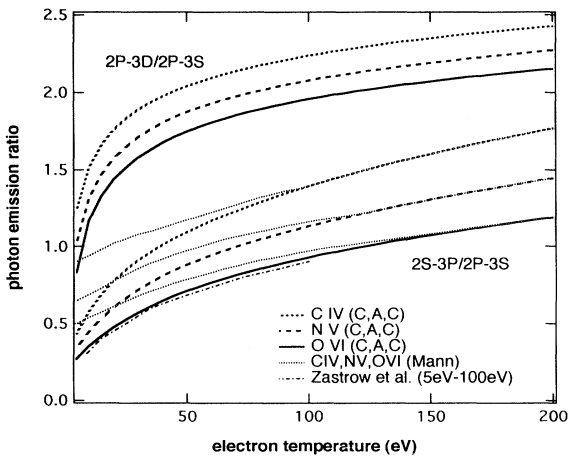

FIG. 3. Photon emission ratios from lithiumlike carbon, nitrogen and oxygen ions for the transitions of $2\,^2P-3\,^2D$ to $2\,^2P-3\,^2S$ and $2\,^2S-3\,^2P$ to $2\,^2P-3\,^2S$. The electron density is assumed to be $n_e=10^{13}$ cm^{-3}. We compare the calculation results for the two different $2\,^2S-3\,^2P$ excitation cross sections in [2].

B. Recombining plasma component

We take Al XI ion as an example. The n_e dependence of the populations of the $n=3$, 4, and 5 levels are shown in Fig. 6 in [2]. In Figs. 4(a) and 4(b) we show the n_e dependence of the magnitude of the population flows divided by n_e for the $4\,^2P$ level. In lower density regions than $n_e=10^{14}$ cm^{-3} ($\eta < 10^7$ cm^{-3}), these excited levels in Fig. 6 in [2] are in the capture-radiative-cascade phase, in which they are populated predominantly by the direct radiative recombination plus cascade, and depopulated through the radiative decay. It may be interesting to remember that, in the case of hydrogen, the contributions from the direct recombination and the cascade are approximately 2:1 [1]. As Fig. 6 in [2] shows, the $n\,^2S$ level has the largest population per unit statistical weight among the different l levels for $n=3$, 4, and 5. At this temperature, the radiative recombination rate coefficient into the s, p, and d levels are approximately proportional to their statistical weights (that for s is slightly smaller) and those for f and especially g are much smaller. The $n\,^2S$ level has the smallest decay probability, resulting in the largest population. The $n\,^2D$ level has the largest radiative decay probability among the same n levels, resulting in the smallest population per unit statistical weight. In the intermediate density region 10^{15} cm$^{-3} < n_e < 10^{19}$ cm^{-3} (10^8 cm$^{-3} < \eta < 10^{12}$ cm^{-3}), the populations of the levels with the same n converge with each other by the l-changing collisions, and they approach the high-density limit values.

In the high-density limit, there is a different characteristic from the ionizing plasma case; as seen in Fig. 4 the net upward or downward flow for $4\,^2S \leftrightarrow 4\,^2P \leftrightarrow 4\,^2D$ is less than 0.1% of the individual flow. This is consistent with the near Boltzmann distribution of these levels as shown in Fig. 2: the same slope of these populations to the Saha-Boltzmann distribution. A similar feature is seen for $4\,^2P \leftrightarrow n \geq 5$ levels (0.5% is the net flow). For $4\,^2P \leftrightarrow n=2$ and 3, however, the net downward population flow is substantial. This suggests that thermal equilibrium would be established for the $n \geq 4$ levels but not with the $n=2$ and 3 levels. This is actually the case, as seen in Fig. 2.

The overall population distribution in Fig. 2 is interpreted. We introduce Byron's boundary in high-density plasma [1,8]; this gives the boundary between the levels in LTE and those for which the ladderlike deexcitation mechanism is established. This boundary is given approximately by

$$p_B^* = \left[\frac{(z-2)^2 R}{3kT_e} \right]^{1/2}, \tag{4}$$

where R is 1 Ry (13.6 eV) and kT_e is the temperature in eV. For levels with principal quantum number p lying above this, the collisional excitation to the $p+1$ level is more frequent than deexcitation to the $p-1$ level, and for levels below that the relation is reversed. Under these

plasma conditions, $p_B^* \cong 4.2$. The population distribution in the ladderlike deexcitation mechanism for $p \lesssim p_B$ has been shown for hydrogen to be given approximately by $n(p^*)/g(p^*) \propto p^{*-6}$. This is based on characteristics of the deexcitation rate coefficient similar to that for the excitation rate coefficient mentioned above. Appendix B shows that, in Fig. 2, the curve representing the Saha-Boltzmann distribution (SB) has slope -6 at $p^* = p_B^*$. The overall population distribution is therefore given by the curve SB for $p^* \geq p_B^*$, and by its linear extrapolation for $p^* \leq p_B^*$ with the slope -6. In Fig. 2, populations of the levels $p \geq 3$ are well approximated by this simple relationship. The gross deviation of $n(2\,^2P)$ from this line is the result of the failure of the approximation for the deexcitation rate coefficients from this level, $F(2\,^2P, 2\,^2S)$.

An important application of the recombining plasma is the x-ray laser of the recombining plasma scheme. In the following we ignore the two factors important in the actual situation but outside the scope of the present study, i.e., the radiation trapping and the transitions involving doubly excited berylliumlike ions [9]. Figure 6 in [2] shows that in the region of $n_e \leq 2 \times 10^{19}$ cm^{-3}, the population inversion is established between the $3\,^2P$ or $3\,^2D$ levels and $n = 4$ or 5 levels. The heliumlike aluminum ion density has been assumed to be 10% of n_e, and the ion temperature to be equal to T_e. We assume the thermal Doppler broadening and the absolute amplification gain is given as

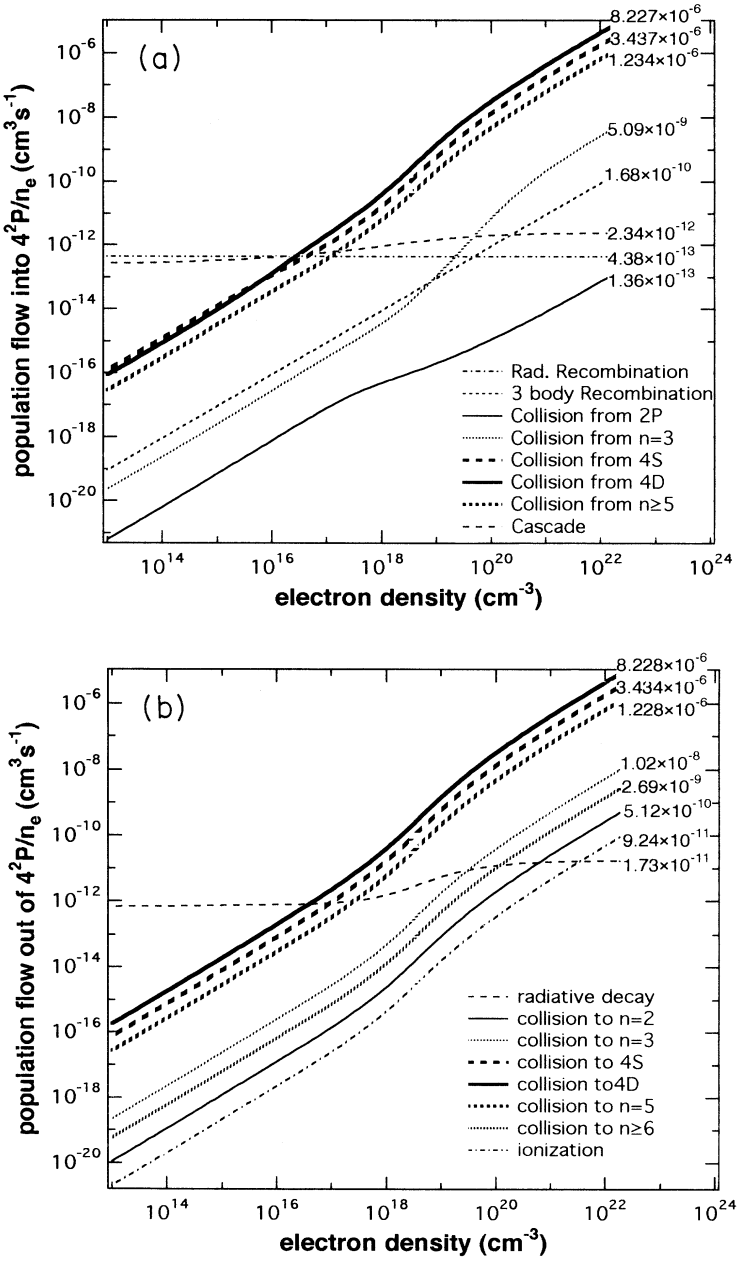

FIG. 4. Population flows (a) into and (b) out of the $4\,^2P$ level for the recombining plasma component in Fig. 6 in [2]. The magnitude of the flow has been divided by electron density for convenience. The number attached on the right side is the magnitude at the high density limit.

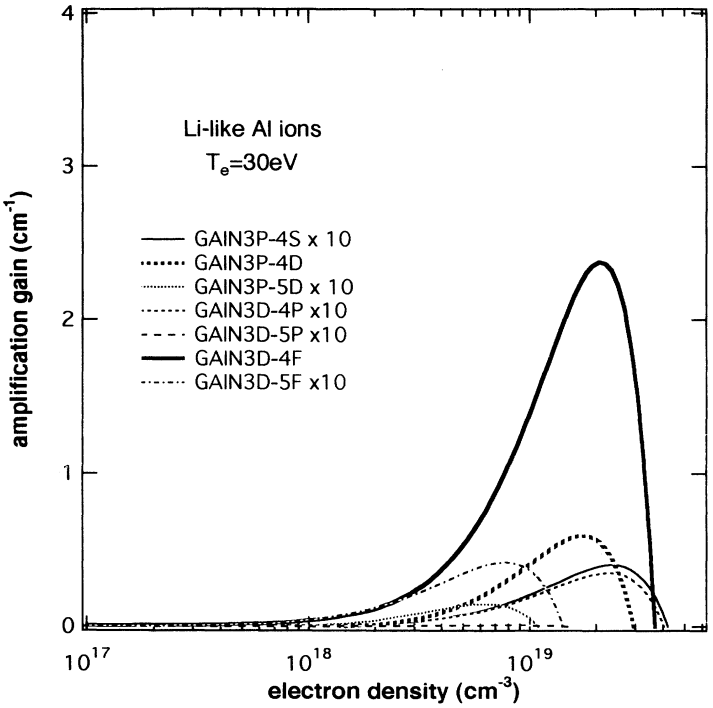

FIG. 5. Absolute amplification gain for lithiumlike aluminum ions. All the gains have been multiplied by 10 except for those for the $3\,^2P-4\,^2D$ and $3\,^2D-4\,^2F$ transitions.

$$\mathcal{G}=(8\pi c)^{-1}\left[\frac{Mc^2}{2\pi kT_e}\right]^{1/2}\left[n(p)-\frac{g(p)}{g(q)}n(q)\right]A(p,q)\lambda^3\ , \tag{5}$$

where p and q are the upper and lower levels, respectively, and M, $A(p,q)$, and λ are the mass of the ion, Einstein's A coefficient and the wavelength of the transition line, respectively. We resolve the levels into fine structure components. Hyperfine structure (nuclear spin of aluminum is $I=\frac{5}{2}$) is neglected. We take the strongest line among the fine structure component levels in our calculation of the gain.

Figure 5 shows the n_e dependence of the gain for $3\,^2D-4\,^2F$, $-5\,^2F$, $-4\,^2P$, $-5\,^2P$, $3\,^2P-4\,^2D$, $-5\,^2D$, $-4\,^2S$, and $3\,^2P-5\,^2S$ lines of Al XI ions. Although population inversion is realized between many pairs of levels in the low-density regions of $n_e \leq 10^{19}$ cm^{-3}, the amplification gain for many of them is very small. Only the two transitions $3\,^2D-4\,^2F$ and $3\,^2P-4\,^2D$ show substantial gain at about $n_e=10^{19}$ cm^{-3}. Carillon *et al.* [10] measured the gain in a laser-produced aluminum plasma. They found that four transitions $3\,^2D-4\,^2F$, $-5\,^2F$, $3\,^2P-4\,^2D$, and $-5\,^2D$ had significant gain; gains of the $3\,^2D-5\,^2F$, $3\,^2P-4\,^2D$, and $3\,^2P-5\,^2D$ transitions were about equal, and that of the $3\,^2D-4\,^2F$ transition was about as twice as large as those of the other three transitions.

Our results for the gain of $3\,^2D-4\,^2F$ and $3\,^2P-4\,^2D$ are smaller than those of the experimental result [10] by a factor of 2, and the gain of $3\,^2P-5\,^2D$ and $3\,^2D-5\,^2F$ are more than ten times smaller. The calculation by Klisnick *et al.* [11] is in accordance with our result. If we assume the calculated populations for the $n=3$ levels, in order

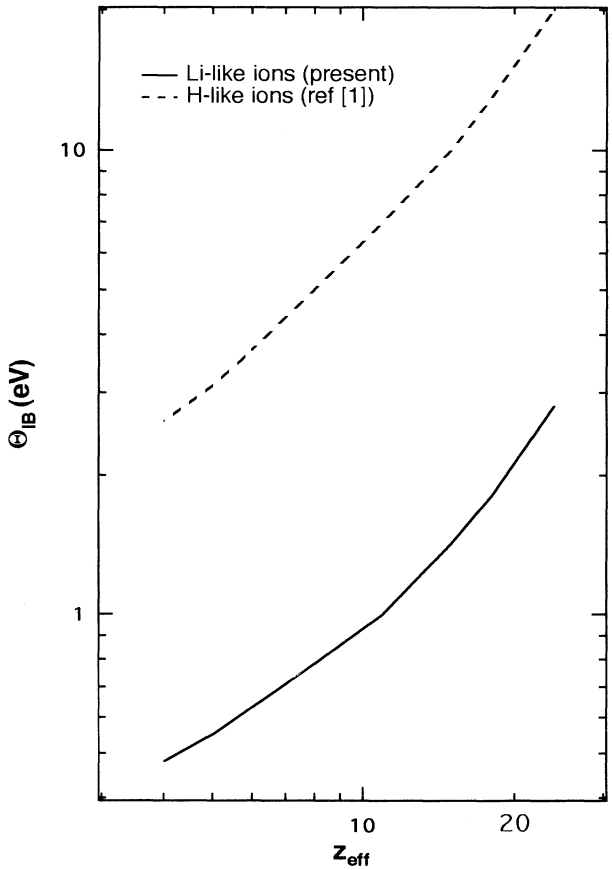

FIG. 6. Optimum temperature is shown as functions of effective nuclear charge $z_{\rm eff}$, where $z_{\rm eff}=z-2$ for lithiumlike ions, and $z_{\rm eff}=z$ for hydrogenic ions.

for our calculated gain to be consistent with experiment the $4\,^2D$ population should be larger by 20% and the $5\,^2D$ and $5\,^2F$ populations by an order. As shown in Fig. 6 in [2] and Fig. 2, under experimental conditions the $n=5$ levels are almost in LTE, and the $n=4$ levels are close to that. Therefore, larger populations, especially in the $n=5$ levels, are unlikely.

C. Ionization balance, ionizing, and recombining plasmas

Ionization balance (IB) is defined as

$$S_{\text{eff}} n_e n_{\text{Li}} = \alpha_{\text{eff}} n_e n_{\text{He}} , \tag{6}$$

where the effective ionization and recombination rate coefficients α_{eff} and S_{eff} are defined in Eq. (3) in [2]. The temperature at which Eq. (6) leads to $n_{\text{He}}=n_{\text{Li}}$ is called the optimum temperature T_{IB} or $\Theta_{\text{IB}}=T_e/z_{\text{eff}}^2$. Figure 6 shows the z_{eff} dependence of the optimum temperature for a low density of $\eta=10^8$ cm^{-3}, and the corresponding temperature for hydrogenic ions [1]. The optimum temperatures for lithiumlike ions are about a factor 5 lower than those for the hydrogenic ions.

It has been shown that, for hydrogen atoms and hydrogenic ions in low-density plasma, the recombining plasma component in Eq. (1) is of the order of 0.1 of that of the ionizing plasma component [1].

We now discuss the relative contributions for the lithiumlike ions. We first limit our discussion to the low-density and high temperature cases, but low enough so that dielectric recombination can be neglected. Equation (6) reduces to

$$S(2\,^2S) n_e n_{\text{Li}} = \sum_p \beta(p) n_e n_{\text{He}} , \tag{7}$$

where S and β mean the ionization rate coefficient and the radiative recombination rate coefficient, respectively. The population ratio between the ionizing and recombining plasma components is approximately given by

$$\frac{n_{\text{He}}\beta(p)}{n_{\text{Li}} C(2\,^2S,p)} = \frac{S(2\,^2S)}{\sum_p \beta(p)} \frac{\beta(p)}{C(2\,^2S,p)} = \frac{S(2\,^2S)}{C(2\,^2S,3)} \frac{C(2\,^2S,3)}{c(2\,^2S,p)} \frac{\beta(p)}{\sum_p \beta(p)} , \tag{8}$$

where 3 is the principal quantum number. In Eq. (8), in the case of the O VI ions, $S(2\,^2S)/C(2\,^2S,3)\approx 0.2$ for $T_e=50$ eV. The last factor may be approximated by

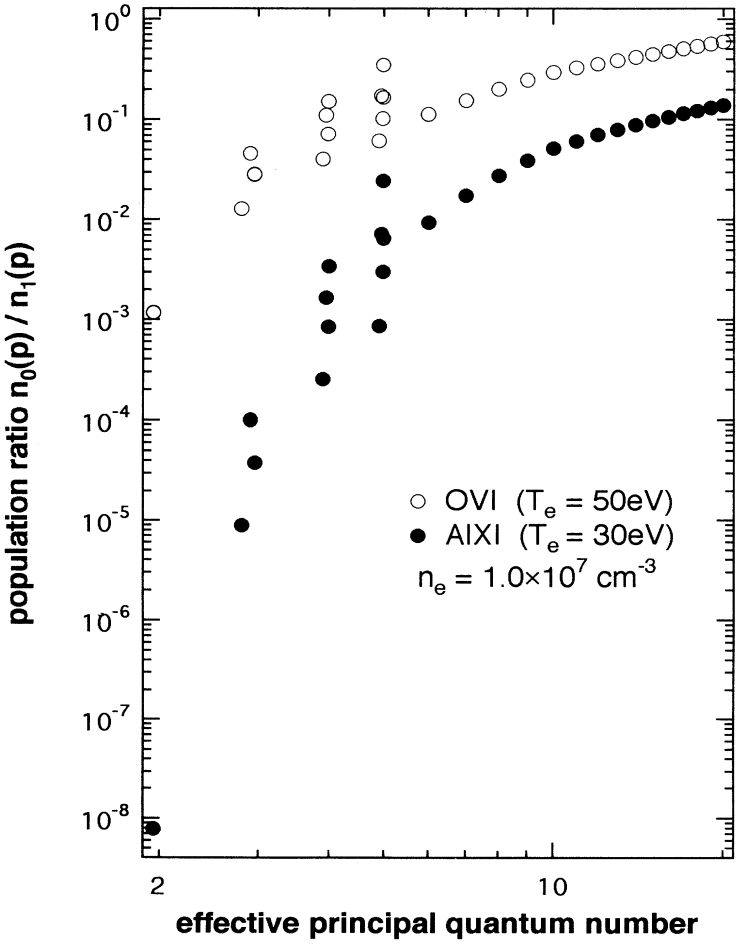

FIG. 7. The ratios of the recombining plasma component to the ionizing plasma component. $T_e=50$ eV and $n_e=1.0\times10^7$ cm^{-3} for O VI, open circle; $T_e=30$ eV and $n_e=1.0\times10^7$ cm^{-3} for Al XI, closed circle.

$\beta(p)/\sum_p \beta(p) \approx p^{-3}/0.2$. $C(2^2S,3)/C(2^2S,p)$ is approximated by $3.5\times 3^{-3}/p^{-3}$ for high-lying levels ($n \geq 7$). The population ratio would be about 3.5×3^{-3} ($=0.13$) for these levels.

Figure 7 shows the calculated population ratios in ionization balance. n_e is assumed to be 10^7 cm^{-3}. In the case of O VI ($\Theta = 1.4$ eV), the ratio is $n_{\rm He}/n_{\rm Li} = 49$. It is concluded that, for the condition of $n_{\rm He}/n_{\rm Li} < 10$ (i.e., the ionizing plasma), the ionizing plasma component in Eq. (1) predominates over the recombining plasma component by more than a factor 10 for all the excited levels. For recombining plasma of $n_{\rm He}/n_{\rm Li} > 5\times 10^5$, the situation is reversed. For ionization balance plasma in the high-density limit, it has been shown [1] that, in Eq. (1), both components together constitute the LTE population (the Saha-Boltzmann distribution against $n_{\rm He}$ and the Boltzmann distribution against $n_{\rm Li}$, in the present case). Figure 2 thus shows the relative contribution from the ionizing plasma component, i.e., $r_1(p)$, and that from the recombining plasma component is given by $[1-r_1(p)]$. It is straightforward to estimate for plasmas out of ionization balance the relative magnitude of both the contributions.

Figure 7 contains the ratios for low temperature (Al XI $T_e = 30$ eV, $\Theta = 0.25$ eV). The ratio is $n_{\rm He}/n_{\rm Li} = 2.5\times 10^{-6}$. Even for recombining plasma of $n_{\rm He}/n_{Li} > 2.5\times 10^{-6}$, the ionizing plasma component tends to persist especially for low-lying levels. For a strongly recombining plasma with $n_{\rm He} = n_{\rm Li}$, for example, the population $n(2^2P)$ is determined by the ionizing plasma component as given in Fig. 5 in [2]. For ionization balance plasma in the high-density limit, a similar argument to the above indicates that, in Fig. 2, the population (the recombining plasma component) with respect to the curve SB gives the relative contribution from the recombining plasma component, and that from the ionizing plasma component corresponds to the difference between the curve and the actual population.

APPENDIX A: CONTRIBUTION FROM CASCADE

We assume hydrogenic ions for the purpose of simplifying the argument. The excitation rate coefficient from the ground state is approximately given as

$$C(1,q) \cong C_0 q^{-3} , \tag{A1}$$

with a constant C_0 and the principal quantum number q. The radiative decay rate from level q is expressed by using a constant H [$=(2^8/3\sqrt{3})\pi e^2 z^4 R^2/h^2 mc^3$]:

$$\sum_{k=1}^{q-1} A(q,k) \cong \int_1^{q-1} \frac{H}{q^3 k(q^2-k^2)} dk$$

$$= \frac{H}{2q^5} \ln\left[\frac{(2q-1(q+1)}{q-1}\right] \cong Hq^{-4.5} . \tag{A2}$$

In the low-density ionizing plasma or in the corona phase, the population of level q is approximately given as

$$n(q) = \frac{C(1,q) n_e n(1)}{\sum_{k<q} A(q,k)} \cong \frac{C_0}{H} q^{1.5} n_e n(1) , \tag{A3}$$

where a cascade contribution has been neglected. The cascading population flow from levels q to p is

$$n(q) A(q,p)$$

and the total cascading flow from all the levels q ($>p$) is

$$\begin{aligned}
\mathcal{F}_{\rm cascade} &\cong \int_{p+1}^{\infty} n(q) A(q,p) dq \\
&\cong \int_{p+1}^{\infty} \frac{C_0 n_e n(1)}{p q^{1.5}(q^2-p^2)} dq \\
&= \frac{C_0 n_e n(1)}{p^2} \left[\frac{2}{p\alpha} + \frac{1}{2p\sqrt{p}} \ln\left[\frac{\alpha-\sqrt{p}}{\alpha+\sqrt{p}}\right] + \frac{1}{p\sqrt{p}} \arctan\frac{\alpha}{\sqrt{p}}\right]_{\alpha=\sqrt{p+1}}^{\infty} \\
&= \frac{C_0 n_e n(1)}{p^3} \left[\frac{\pi}{2\sqrt{p}} - \frac{2}{\sqrt{p+1}} - \frac{1}{2\sqrt{p}} \ln\left[\frac{\sqrt{p+1}-\sqrt{p}}{\sqrt{p+1}+\sqrt{p}}\right] - \frac{1}{\sqrt{p}} \arctan\frac{\sqrt{p+1}}{\sqrt{p}}\right] .
\end{aligned} \tag{A4}$$

By using Eqs. (A1) and (A4), we obtain the relative contribution ζ from the cascading to the population flow into level p,

$$\begin{aligned}
\zeta &= \frac{\mathcal{F}_{\rm cascade}}{C(1,p) n_e n(1) + \mathcal{F}_{\rm cascade}} \\
&= \frac{\left[\frac{\pi}{2\sqrt{p}} - \frac{2}{\sqrt{p+1}} - \frac{1}{2\sqrt{p}} \ln\left[\frac{\sqrt{p+1}-\sqrt{p}}{\sqrt{p+1}+\sqrt{p}}\right] - \frac{1}{\sqrt{p}} \arctan\frac{\sqrt{p+1}}{\sqrt{p}}\right]}{1+\left[\frac{\pi}{2\sqrt{p}} - \frac{2}{\sqrt{p+1}} - \frac{1}{2\sqrt{p}} \ln\left[\frac{\sqrt{p+1}-\sqrt{p}}{\sqrt{p+1}+\sqrt{p}}\right] - \frac{1}{\sqrt{p}} \arctan\frac{\sqrt{p+1}}{\sqrt{p}}\right]} .
\end{aligned} \tag{A5}$$

The values of ζ for $p=4$, 6, and 10 is 0.187, 0.190, and 0.193, respectively. If we take into account the cascade contribution in Eq. (A3), ζ would be slightly larger than 20%.

APPENDIX B: POPULATION DISTRIBUTION OF HIGH-DENSITY RECOMBINING PLASMA

The Saha-Boltzmann population for lithiumlike ions with nuclear charge z is

$$n(p)=\frac{g(p)}{2g_{\mathrm{He}}}\left[\frac{h^2}{2\pi mkT_e}\right]^{3/2}\exp\left[\frac{(z-2)^2R/p^{*2}}{kT_e}\right], \tag{B1}$$

where p^* is the effective principal quantum number and R is 1 Ry. We express $n(p)$ and p^* in a common logarithmic scale (see Fig. 2) and transform Eq. (B1) to

$$\log_{10}\frac{n(p)}{g(p)}=\log_{10}\frac{1}{2g_{\mathrm{He}}}\left[\frac{h^2}{2\pi mkT_e}\right]^{3/2}+\frac{1}{t}\left[\frac{(z-2)^2R}{kT_e}\exp(-2t\alpha)\right] \tag{B2}$$

where

$$t=\log_e 10, \quad \alpha=\log_{10}p^* . \tag{B3}$$

We differentiate Eq. (B2) with α:

$$\frac{d}{d\alpha}\left[\log_{10}\frac{n(p)}{g(p)}\right]=-2\frac{(z-2)^2R}{kT_e}\exp(-2t\alpha) . \tag{B4}$$

At Byron's critical level p_B^*, Eq. (4) is expressed as

$$\left[\frac{(z-2)^2R}{3kT_e}\right]^{1/2}=\exp(t\alpha) . \tag{B5}$$

Substitution of Eq. (B5) into Eq. (B4) yields a slope -6 at $p^*=p_B^*$.

[1] T. Fujimoto, J. Phys. Soc. Jpn. **47**, 265 (1979); **47**, 273 (1979); **49**, 1561 (1980); **49**, 1569 (1980); **54**, 2905 (1985).

[2] T. Kawachi, T. Fujimoto, and G. Csanak, preceding paper, Phys. Rev. E **51**, 1428 (1995).

[3] D. H. Sampson, J. Phys. B **10**, 749 (1977).

[4] T. Fujimoto, Y. Ogata, I. Sugiyama, K. Tachibana, and K. Fukuda, Jpn. J. Appl. Phys. **12**, 718 (1972).

[5] K. Tachibana and K. Fukuda, Jpn. J. Appl. Phys. **12**, 895 (1973).

[6] A. Hirabayashi, Y. Nambu, M. Hasuo, and T. Fujimoto, Phys. Rev. A **37**, 77 (1988).

[7] K-D. Zastrow, J. H. Brzozowski, E. Källne, and H. P. Summers, Report No. TRITA-PFU-91-09, Stockholm (1991) (unpublished).

[8] S. Byron, R. C. Stabler, and P. I. Bortz, Phys. Rev. Lett. **8**, 376 (1962).

[9] T. Fujimoto and T. Kato, Phys. Rev. A **32**, 1663 (1985); **35**, 3024 (1987); Phys. Rev. Lett. **48**, 1022 (1982).

[10] A. Carillon, M. J. Edwards, M. Grande, M. J. de C. Henshaw, P. Jaegle, G. Jamelot, M. H. Key, G. P. Kiehn, A. Klisnick, C. L. S. Lewis, D. O'Neill, G. J. Pert, S. A. Ramsden, C. M. E. Regan, S. J. Rose, R. Smith, and O. Willi, J. Phys. B **23**, 147 (1990).

[11] A. Klisnick, A. Sureau, H. Guennou, C. Moller, and J. Virmont, Appl. Phys. B **50**, 153 (1990).